

## **HYDROGEN EMBRITTLEMENT OF HIGH STRENGTH STEELS BY PHASE TRANSITIONS**

**JAVIER SANCHEZ\*, PEDRO DE ANDRES†, ALEJANDRO CASTEDO\*, CARMEN ANDRADE\*, JOSE FULLEA\***

\* Centro de Seguridad y Durabilidad Estructural y de Materiales. Instituto de Ciencias de la Construcción Eduardo Torroja (CISDEM-IETcc-CSIC-UPM).  
C/ Serrano Galvache, 4 - 28033 Madrid, Spain  
e-mail: alejandro.castedo@estudiante.uam.es, javiersm@ietcc.csic.es, andrade@ietcc.csic.es, fullea@ietcc.csic.es

† Instituto de Ciencias de Materiales de Madrid (ICMM-CSIC).  
E-28049 Cantoblanco, Madrid, Spain  
Email: pedro.deandres@csic.es

**Key words:** Ab-Initio, Hydrogen Embrittlement, High Strength Steel

**Abstract:** Hydrogen embrittlement is believed to be one of the main reasons for cracking of steel structures under stress and stress corrosion cracking process. To control and prevent the cracking of steel it is necessary to understand the chemical and physical properties of hydrogen inside iron. Usually, pre-stressed steels are high strength steels that include a ferritic core made of  $\alpha$ -iron (body-centered-cubic lattice, bcc). Previous works have focused on the effect of internal and external stresses/strains on the interstitial H and bcc-Fe interaction. Using ab-initio Molecular Dynamics and by taking statistical averages diffusion coefficients for hydrogen diffusion paths have been obtained. Depending on temperature, the diffusion path visits preferentially tetrahedral or octahedral sites. Simulations where a number of hydrogens occasionally meet in one unit cell have been performed to elucidate the effect of interactions between hydrogens, and diffusion coefficients have been calculated from Einstein's equation. Under these conditions, the Fe-Fe interaction has been found to be weaker than in the absence of hydrogen. Debye temperature for Iron decreases monotonically with and increasing concentration of interstitial hydrogen, showing that iron-iron interatomic potential is weaker in the presence of a large number of diffusing hydrogen atoms. In this work, we have focused on the structural consequences for the iron lattice upon absorption of interstitial H in octahedral sites. Using ab-initio Density Functional Theory we have computed the kinetic barriers for a phase transition  $bcc > fcc > hcp$  along a Bain's pathway. All the barriers are lowered by the presence of hydrogen; the initial part ( $bcc > fcc$ ) being almost barrierless. This kind of phase transformation carries out atomic rearrangements and changes in the unit cell volume that should affect the mechanical properties of iron, as revealed by calculations for the elastic constants of the material.

### **1 INTRODUCTION**

Hydrogen embrittlement is believed to be one of the main reasons for cracking of steel structures under stress [1-4]. Pearlitic cold-drawn wires and strands are the active tendons

in prestressed concrete structures. The word estimated production of pearlitic-drawn wire is more than 25 million tons per year [5]. Pearlitic steels have a ferrite matrix with cementite lamellas. The ferritic core is made of

$\alpha$ -iron (body centred cubic lattice, BCC). To control and prevent the cracking of steel it is necessary to understand the chemical and physical properties of hydrogen inside BCC iron. These results are critical to use as set parameters in modeling H embrittlement and should help suggest engineering solutions. Hydrogen absorbed in iron has been studied from different approaches, both from a theoretical and experimental point of view. Unfortunately, a clear consensus about fundamental questions, like the nature of the equilibrium absorption site, the reasons for H to prefer some regions over others, or how to modify the diffusion barriers has not been reached. Many theoretical papers have favoured hydrogen absorbed in the tetrahedral site (T) [6-9], some have preferred the octahedral one (O) [10], others have reported that they are almost equivalent [11] (Fig. 1). From an experimental point of view, it is generally believed that hydrogen has low solubility and high mobility in bcc-iron. However, some experiments have attained high concentrations [12-15], have concluded that hydrogen partly occupies the O-site, or have measured diffusion barriers that depend on the amount of H admitted into the material [16].

We simulate the atomic absorption and diffusion of hydrogen in the body centred cubic iron lattice from first-principles [17, 18]. Absorption in high-symmetry sites for different hydrogen loads (densities) has been explored and the internal strains/stresses have been calculated. Diffusion barriers between these stationary absorption sites have been obtained, and the effect of external stresses on diffusion coefficients has been analyzed.

In this paper, firstly we show the dynamical behaviour of hydrogen inside the iron lattice. Using ab-initio Molecular Dynamics we obtain hydrogen diffusion paths and by taking statistical averages diffusion coefficients. Depending on temperature, the diffusion path involve going through tetrahedral or octahedral. Simulations where a number of hydrogens occasionally coincide in one unit cell have been performed to elucidate the effect of interactions between hydrogens.

From simulated diffusion path we extract the diffusion coefficient from Einstein's equation. We also show the Fe-Fe interaction weakens. Iron Debye temperature decreases monotonically for increasing concentration of interstitial hydrogen, proving that iron-iron interatomic potential is significantly weakened in the presence of a large number of diffusing hydrogen atoms.

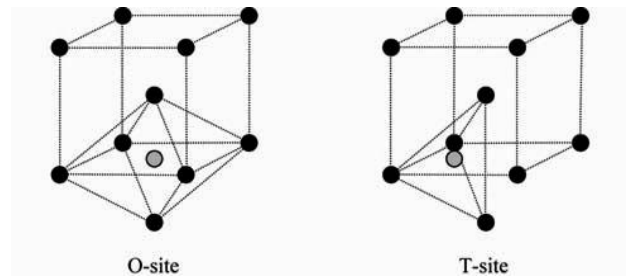


**Figure 1:** High symmetry sites for H absorption inside  $\alpha$ -iron: the octahedral (O) and tetrahedral (T) sites (grey) are shown along with iron atoms in the BCC lattice (black).

Finally, we show the possible structural changes of the lattice that might be produced by the tetragonal distortion induced by hydrogen. There are several known phases of iron reported in literature. Experimental work shows three main phases: bcc iron ( $\alpha$ -iron), fcc iron ( $\gamma$ -iron) and hcp iron ( $\epsilon$ -iron). These three phases are shown in Figure 2. Bain's pathway [19] offers an elegant and easy to understand mechanism for the martensitic transformation between  $\alpha$ -iron and  $\gamma$ -iron. If we name  $a$ ,  $b$  and  $c$  the axes of our unit cell (UC) we can explain this mechanism in terms of the change in the  $a/c$  ratio ( $a = b$  throughout the whole process). The tetragonal distortion consists of a contraction upon two of the cubic axes ( $a$  and  $b$ ) and a continuous expansion along the third one ( $c$ ). When the value  $\sqrt{2}$  is reached the configuration of the system now matches that of the fcc iron. Our calculations go up to a  $c/a = 1.6$  where the hcp stable phase of iron has been found, although the mechanism that transforms fcc into hcp differs from that of Bain, since we no longer find the UC in the bcc regime (one angle of the UC deforms to reach  $60^\circ$ ) and it can be explained by a shear and a shuffle. This is the actual unit cell used in the calculations, a bcc cell that consists of 2 atoms

(or 3 in the case when we add hydrogen).

Bain's path is not the only transformation suggested in literature to explain this phase changes but it is preferable for a number of reasons: (i) it retains the highest possible crystal symmetry throughout the process, (ii) it is simple, and (iii) it contains the lattice deformation expected for hydrogen occupation of (O-site) interstitials.



Figure 2: Bcc, fcc and hcp structures.

## 2 METHODOLOGY

First-principles molecular dynamics (MD) calculations have been performed with the CASTEP code [20]. A  $2 \times 2 \times 2$  periodic supercell is set up including 16 Fe atoms and several H atoms depending on the different concentrations being considered. The Born-Oppenheimer approximation is used; ions are considered classical objects moving on the potential created by the electrons obeying the Schrödinger equation. Electronic wave functions are expanded using a plane-wavebasis set up to an energy cutoff of 375 eV and are sampled inside the Brillouin zone in a  $4 \times 4 \times 4$  Monkhorst-Pack mesh [21]. Electronic energies are converged up to  $10^{-5}$  eV. Ultrasoft pseudopotentials are used to describe Fe and H [22] and the generalized gradients approximation for exchange and correlation due to Perdew, Burke, and Ernzerhof is chosen [23]. These approximation have been thoroughly checked before and it has been found that they reproduce correctly the main physical properties of  $\alpha$ -iron, including lattice constant, magnetization, and bulk modulus [18]. The k-point mesh we are using in this Brief Report is less dense than the ones we have previously shown to be adequate to accurately reproduce different equilibrium properties of  $\alpha$ -iron at  $T = 0$  K. Our choice is based in two different reasons. First of all, it is a practical one since Ab-Initio Molecular

Dynamics is a computer intensive task and a compromise between accuracy and time must be made. Second, we notice that computing different physical magnitudes require different accuracies. Figure 2 in [18] shows that a k-point mesh similar to the one we are using here incurs in a fractional error of 0.4% for the equilibrium lattice constant but  $\sim 300\%$  for the bulk modulus. Presently, we focus in the calculation of total energies that fluctuate in the current range of temperatures by  $\sim 0.05$  eV. We have checked that for the maximum density of interstitial impurities considered here the total energy changes at  $T = 0$  K by 0.047 eV if the  $4 \times 4 \times 4$  mesh is replaced by a  $8 \times 8 \times 8$  one. Therefore, the error becomes acceptable because it is similar to the random fluctuations intrinsic to the system. On the other hand, we notice that the error in the equilibrium lattice parameter by introducing such an approximation is  $\sim 0.01$  Å [18], which is of the same order of magnitude or lower than the root-mean-squared amplitude displacements of vibrating atoms at the temperatures used here. Finally, we have checked our ability to reproduce the experimental value for the Debye temperature of bcc iron ( $\Theta = 420$  K), a physical magnitude that will be used below to get physical insight from the molecular dynamics runs. We have obtained a theoretical value of  $\Theta = 505$  K, quite acceptable for our purposes, in particular, because our methodology relies more than on absolute values on interpreting differences in magnitudes computed theoretically with the same parameters where a common background error should tend to cancel. Therefore, we conclude that the  $4 \times 4 \times 4$  mesh is both practical and accurate enough for the purpose of these simulations.

## 3 RESULTS AND DISCUSSION

### 3.1 Hydrogen diffusion in Fe lattice

To study the diffusion of several H atoms inside the unit cell we test in the microcanonical ensemble the quality of the total energy conservation during a typical MD run. Simulations for 1 or 2 ps are performed

with time steps of 0.5 or 1.0 fs showing that the total energy is conserved within a 0.01% error (equilibration taking place during the first 100–200 fs have been taken out from averages). Keeping fixed the parameters defining the model, we switch to the canonical ensemble to reproduce conditions where the Fe and H atoms are in equilibrium with a thermal bath kept at a fixed temperature (Nose-Hover prescription has been used). All these simulations are performed keeping constant the volume of the unit cell and the number of particles. These boundary conditions are important to understand the physical model and the solutions obtained. In particular, it is relevant to discuss the meaning of keeping the volume fixed. In a previous work we have investigated the volume deformation and atomic displacements necessary to find an equilibrium solution with zero forces and stresses in the presence of interstitial hydrogen binding to either the octahedral or tetrahedral high-symmetry sites. Here we are interested, for the case of an overall low dilution concentration of impurities, in the effect of a high concentration of interstitial atoms inside a small region embedded in a matrix of iron that, except for the large concentration of interstitial hydrogen in a small number of regions, mostly keeps its original properties. This is consistent with the experimental observation of overall low dilution of interstitial H in  $\alpha$ -iron, but possibly large concentration in particular regions, maybe as a consequence of the existence of defects [15, 24]. Therefore, we assume that the modification of the volume in the region of interest due to the internal pressure created by the impurities is effectively controlled by the larger amount of unperturbed bulk material surrounding the region where the interstitial hydrogen diffuses in a scale of time compatible with our simulations (ps). Consequently, we keep the simulation  $2 \times 2 \times 2$  supercell volume fixed, equal to the one corresponding to  $\alpha$ -iron. Other models might be of interest for different conditions: e.g., a large and uniform concentration of impurities. This would require adjusting the volume for each density. We estimate that for this case the volume

would change between 5% and 15% in the range of impurity concentrations considered in this work. While the NVE and NVT collectives are appropriate for the first scenario above, for the second one the NPH and NPT collectives should be used.

Diffusion coefficients are computed by assuming a random walk for interstitial impurities. Figure 3 shows the different paths for the high-density case with eight hydrogen atoms diffusing simultaneously inside the  $2 \times 2 \times 2$  supercell. As already predicted by our static geometry optimization interstitial hydrogen atoms avoid each other and no tendency to formation of molecular hydrogen has been observed. We follow the different trajectories during the simulation time and compute averages to extract the three-dimensional diffusion coefficient  $D$ . Barriers for diffusion are estimated from an Arrhenius plot  $D = D_0 e^{-B/kBT}$  by a least-squares fit. Here, the prefactor  $D_0$  is related to a typical vibrational frequency for H in the Fe bcc lattice, and it is assumed to be a constant value independent of the number of interstitial atoms in the supercell. This assumption is corroborated by our fits within an uncertainty of  $\pm 12\%$ .

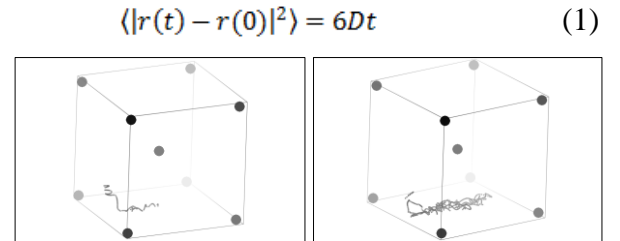


**Figure 3:** Diffusion path: tetrahedral-tetrahedral jump (H/Fe=1/16, T=600 K), and octahedral-octahedral jump (H/Fe=8/16, T=500 K).

We simulate MD trajectories for a single H atom diffusing inside the supercell to compare with previous results derived from ab initio DFT geometrical optimization and transition state theory. From a least-squares fit to the data in the Arrhenius plot we determine a barrier for diffusion  $B1 = 0.145$  eV (Figure 4) in good agreement with previous values obtained under similar conditions [18]. This agreement shows that our MD simulations adequately sample the relevant phase space.

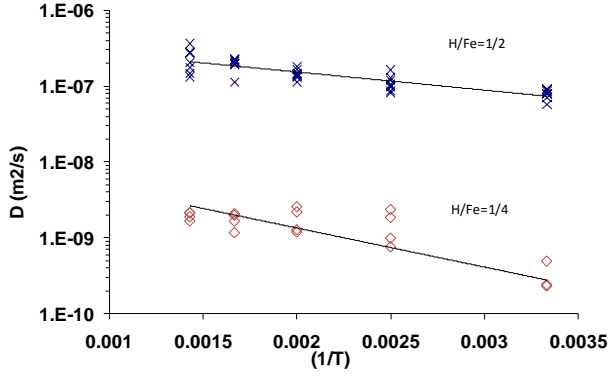


**Figure 4:** Diffusion coefficient,  $D$  ( $\text{m}^2/\text{s}$ ), obtained for a set of diffusion MD trajectories for four H atom in a  $2 \times 2 \times 2$  bcc iron supercell ( $H/\text{Fe} = 1/4$ ). A barrier for diffusion of  $B4 = 0.102$  eV is obtained from a least-squares fit. Same for eight H interstitial atoms diffusing in the supercell ( $H/\text{Fe} = 1/2$ ). A barrier of  $B8 = 0.047$  eV is deduced from the fit.

The time evolution of the interstitial atom can be further analyzed to show that under these conditions trajectories near tetragonal sites (T) are preferred over octahedral sites (O). This conclusion can be made quantitative by computing a characteristic residence time for both sites. We assign parts of the diffusing path either to T or O according to proximity to estimate the likelihood to find the particle, say, near O. Figure 5 displays the fractional occupation of octahedral sites for one, two, four, and eight (H1, H2, H4 and H8) hydrogen atoms in the  $2 \times 2 \times 2$  supercell. These values can be understood by comparing with a simple two-level model where the only parameter is the energy difference between T and O sites,  $k_B \Delta = E_O - E_T$ .

$$\frac{O}{O+T} = \frac{1}{1+2e^{\Delta/T}} \quad (2)$$

This model reduces all the accessible volume for the interstitial hydrogen diffusing in the unit cell to only a set of discrete lattice points (either T or O) but in spite of its crudeness it already captures the essentials of the problem. Equation 2 has been plotted in Figure 5 for  $k_B \Delta = 0.06, 0.07, 0.04,$  and  $-0.035$  eV, yielding least-squares fits to the points extracted from the MD simulations for  $n_H = 1, 2, 4,$  and  $8$  interstitial hydrogen atoms, respectively. The dashed line represents the

asymptotic equilibrium distribution ( $O_{T \rightarrow \infty} = 1/3$ ) to be approached from above or below depending on the sign of  $\Delta$ . These results show that for  $n_H = 8$  has moved from positive to negative and the equilibrium site has been exchanged from T to O. The dependence of the parameter  $\Delta$  with the interstitial density proves how site-adsorption energies are affected by the presence of an increasing number of hydrogen atoms concentrated in a particular region. This behaviour follows the pattern previously predicted by Ab-Initio DFT geometry optimization where the T site is the lowest energy configuration for low densities while for large densities occupancy of the O site favors a body-centered tetragonal distortion of the lattice and becomes the global minimum. Although for the  $\gamma$  phase, experiments reporting a qualitative modification of the system around a hydrogen concentration of  $\sim 0.4$  show how the increasing density of interstitial impurities might significantly modify the dynamics of these systems [25]. This is an observation that might help to explain the spreading of values extracted from different experimental techniques for diffusion barriers that has previously been linked to partial occupation of both sites [16]. Partial occupation of both sites at a given temperature happens most naturally in molecular dynamics simulations but it is not easy to describe in a standard geometry optimization. We remark that the present approach represents a feasible route to investigate a regime that otherwise is too difficult: in the  $2 \times 2 \times 2$  there are 48 different O sites and 96 different T sites, being the number of ways to distribute several interstitial among these combinatorially large ( $\sim 10^{11}$ ). Such a huge configurational space can only be addressed from a statistical point of view and by letting the system to explore as many relevant cases as possible by following its own dynamics. To understand to which extent barriers for diffusion are affected by the presence of extra interstitial atoms we analyze the high-density case  $\Theta = 1/2$  in more detail. From an Arrhenius plot (Figure 4) we extract by a least squares fit an effective barrier of  $B8$

= 0.047 eV; significantly lower than the one found for a single interstitial, B1.

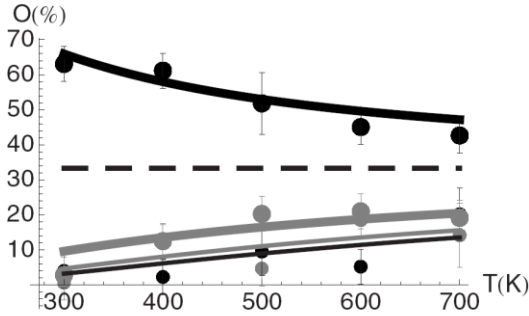


**Figure 5:** As a percentage over the total simulation time, residence time around octahedral sites,  $P_O$  for: (i) a single interstitial hydrogen H1 corresponds to  $k_B\Delta = 0.06$  eV in Eq. 2; (ii) two H ( $k_B\Delta = 0.07$  eV); (iii) four H ( $k_B\Delta = 0.04$  eV); and (iv) eight H ( $k_B\Delta = -0.035$  eV).

Based in ab initio DFT geometrical optimization we have previously suggested that an important consequence of interstitial hydrogen diffusing in  $\alpha$ -Fe is to weaken the Fe-Fe interaction [17, 26]. From a physical point of view this effect is related to several factors: first, interstitial impurities help to screen the Fe-Fe interaction; second, the symmetry is distorted, an effect that is important to explain the stability of octahedral sites versus tetrahedral ones in the high-density regime; third, spin-polarized DFT calculations reveal that hydrogen contributes an extra spin to the system, but the total ferromagnetic moment does not grow accordingly, which we interpret as a weakening of electronic interactions. Current MD simulations should be interpreted as controlled and clean theoretical experiments that help to explore new domains, such as nonzero temperatures, or the collective behaviour of a large number of interstitial impurities meeting together in the same region. We remark that our MD simulations support similar physical interpretations as the ones derived from Ab Initio DFT at  $T = 0$  K. We compute the mean-square amplitudes of iron atoms vibrating around their equilibrium positions,  $\langle u^2 \rangle$ , which is related to the strength of the potential confining these atoms. For each temperature we obtain the mean-squared

amplitude of vibration by fitting their time-averaged probabilities to a Gaussian distribution centred around its equilibrium position. These values are compared with an isotropic Debye-Waller model for the mean-squared displacement of atoms vibrating at temperature T:

$$\langle u^2 \rangle = \frac{3\hbar^2}{4k_B M \Theta} \left( \frac{T}{\Theta} \int_0^{\Theta/T} \frac{x dx}{e^x - 1} + \frac{1}{4} \right) \quad (3)$$

where  $\Theta$  is the Debye temperature and  $M$  the mass of the atom. Figure 6 shows how the root-mean-squared amplitude of vibration  $\langle u \rangle$  increases steadily with the number of H atoms inside the  $2 \times 2 \times 2$  supercell, being nearly doubled from  $n_H = 1$  to 8. Adopting a Lindemann-type criterion we can conclude that increasing the number of interstitial hydrogen drives the material closer to a thermodynamic instability that eventually should lead either to a phase transition or to the material failure. This idea is more clearly illustrated by using Eq. 3 to fit these  $\langle u^2 \rangle$  to an effective Debye temperature for each density (Figure 7).  $\Theta$  decreases monotonously when the number of interstitial hydrogen atoms increases marking the softening of  $\alpha$ -iron and proving that the material is, at a given fixed T, getting closer to its own melting point under the internal pressure of dissolved H. This is closely related to the growing number of interstitial atoms sitting together in the same unit cell. The inverse situation (growing temperature getting closer to the melting point at a fixed number of interstitial impurities) cannot be inferred from our simulations because the Debye Temperature is constant under these conditions.

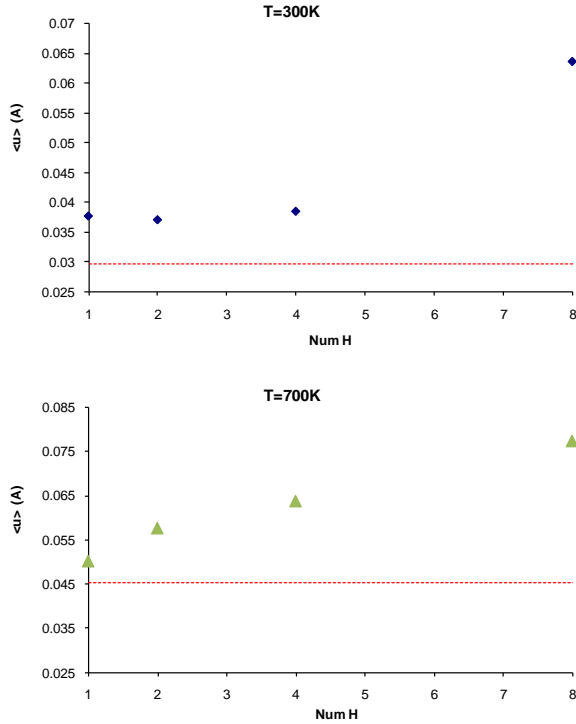


**Figure 6:** Iron root-mean-squared displacement from equilibrium positions  $u$  (Å) vs density of interstitial hydrogen at two temperatures. The horizontal line corresponds to Fe without H.

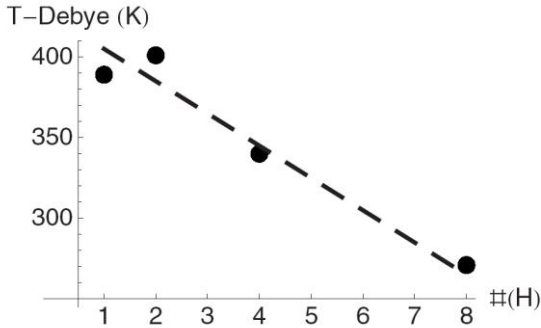


**Figure 7:** Debye-Waller temperature (K) vs number of interstitial H diffusing in the unit cell. Dashed line is a linear least-squares fit to guide the eye.

### 3.2 Hydrogen induced changes in structural properties of iron

Our calculations are performed at the following system conditions,  $T = 0$  K and  $P = 0$  GPa. The global minimum for pure iron (without impurities) is a bcc phase corresponding to a ferromagnetic state,  $c/a = 1$  and all angles  $90^\circ$ . The next minimum found corresponds to a minimum close to a fcc configuration, angles  $90^\circ$  and  $c/a = 1.51$  and it

is an antiferromagnetic (Type I; AF-I) state. The ideal ratio for a fcc phase is  $\sqrt{2} \approx 1.41$  which can be found by our calculations if we consider NM (non magnetic) states. Once we consider the possibility of AF states we realized that an AF-I state would decrease the energy of this specific local minimum, making it the most possible candidate for the local minimum. Further away in the  $c/a$  ratio we find another local minima with an hexagonal configuration (hcp), with  $\gamma = 60^\circ$  and  $c/a \approx 1.6$  that matches the prediction for the ideal ratio of hcp structures as well as experimental examples of this phase. Magnetism is important and in the present work three possible magnetic ordering states have been considered for each minimum; **Non-magnetic (NM)**, **Ferromagnetic (FM)** and **Antiferromagnetic (AF)**. Only the lowest energy states are displayed in the figures that accompany this article.

In the case in which we add hydrogen the picture is qualitatively different. First we notice that hydrogen produces the so mentioned tetragonal distortion of the UC and bcc is no longer a minimum. The system is no longer at an stable configuration and the effect of this internal stress is to drive the system along Bain's path towards a fcc phase first, and subsequently towards an hcp phase that can be reached by a shear and a shuffle of our bct unit cell. This last configuration is the global minimum. We observed that the position of hydrogen slowly varies throughout the process choosing always an O-site, including the hexagonal phase only that this time it is harder to visualize. This behaviour agrees with experimental findings where hydrogen always occupies O-sites in hexagonal-close-packed structures, with no experimental evidence of occupancy of T-sites [12]. These experimental findings are also a good evidence of high density hydrogen systems.

The interpretation of the results obtained by our calculations has been summarized in Figure 8 and Figure 9. Table 1 gives actual numerical values compared to those available from experimental works. Our calculations are performed at the following system conditions,  $T = 0$  K and  $P = 0$  GPa. The global minimum

for pure iron (without impurities) is a bcc phase corresponding to a ferromagnetic state,  $c/a = 1$  and all angles  $90^\circ$ . The next minimum found corresponds to a minimum close to a fcc configuration, angles  $90^\circ$  and  $c/a = 1.51$  and it is an antiferromagnetic (Type I; AF-I) state. The ideal ratio for a fcc phase is  $\sqrt{2} \approx 1.41$  which can be found by our calculations if we consider NM (non magnetic) states. Once we consider the possibility of AF states we realized that an AF-I state would decrease the energy of this specific local minimum, making it the most possible candidate for the local minimum. Further away in the  $c/a$  ratio we find another local minima with an hexagonal configuration (hcp), with  $\gamma = 60^\circ$  and  $c/a \approx 1.6$  that matches the prediction for the ideal ratio of hcp structures as well as experimental examples of this phase. Magnetism is important and in the present work three possible magnetic ordering states have been considered for each minimum; Non-magnetic (NM), Ferromagnetic (FM) and Antiferromagnetic (AF). Only the lowest energy states are displayed in the figures that accompany this article.

In the case in which we add hydrogen the picture is qualitatively different. First we notice that hydrogen produces the so mentioned tetragonal distortion of the UC and bcc is no longer a minimum. The system is no longer at an stable configuration and the effect of this internal stress is to drive the system along Bain's path towards a fcc phase first, and subsequently towards an hcp phase that can be reached by a shear and a shuffle of our bct unit cell. This last configuration is the global minimum. We observed that the position of hydrogen slowly varies throughout the process choosing always an O-site, including the hexagonal phase only that this time it is harder to visualize. This behaviour agrees with experimental findings where hydrogen always occupies O-sites in hexagonal-close-packed structures, with no experimental evidence of occupancy of T-sites [12, 27]. These experimental findings are also a good evidence of high density hydrogen systems.

The interpretation of the results obtained by our calculations has been summarized in

Figure 8 and Figure 9. Table 1 gives actual numerical values compared to those available from experimental works.

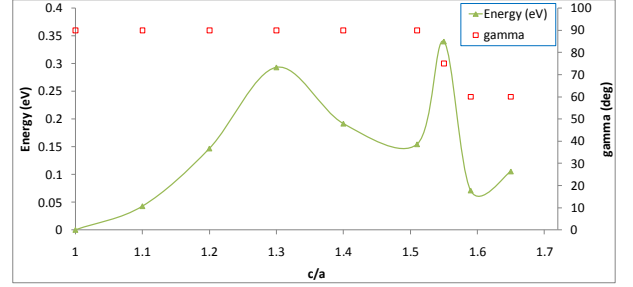


**Figure 8:** Total energy along Bain's path for pure iron parameterized by the value  $c/a$ . The values of the angle  $\gamma$  is indicated above.

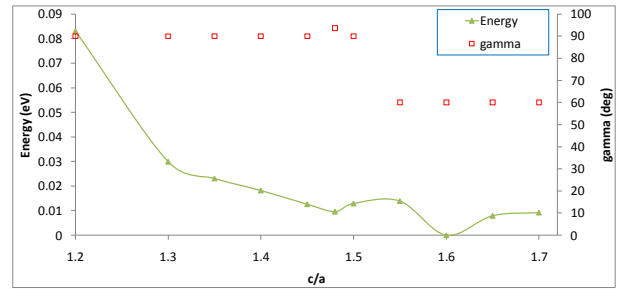


**Figure 9:** Same as 8 but for the system with hydrogen.

**Table 1:** Comparison of theoretical and experimental parameters. Distances are given in  $\text{\AA}$ , enthalpies in eV and spin in  $\mu\text{B}$

<b>Clean Fe</b>	$a(\text{\AA})$	$c/a$	$\mu\text{B}$	$\text{vol}(\text{\AA}^3)$
BCC-Teor	2.82	1.00	2.20	22.33
BCC-Exp[28]	2.87	1.00	2.20	2.80
FCT-Teor	2.43	1.50	0.00	20.27
FCC-Exp[28]	2.55	1.42	0.00	-
HCP-Teor	2.45	1.58	0.00	22.16
HCP-Exp[12]	2.58	1.62	0.00	-
<hr/>				
<b>Fe+H</b>	$a(\text{\AA})$	$c/a$	$\mu\text{B}$	$\text{vol}(\text{\AA}^3)$
HCP-Teor	2.52	1.60	0.00	22.13

## 12 CONCLUSIONS

We have found by direct analysis of our MD trajectories that the diffusing barrier for interstitial hydrogen inside  $\alpha$ -iron depends on the density of diffusing atoms in the near

region. By using a simple statistical model we have also analyzed how the energy difference between the T and O sites,  $\Delta$ , is modified by the presence of other interstitials. Finally, by looking at the amplitude of vibration of iron atoms around their equilibrium position and comparing with a simple Debye-Waller model, we conclude that the Fe-Fe interaction weakens as the concentration of interstitial hydrogen increases, finding that for the largest considered density the effective Debye temperature for iron is already below room temperature.

Calculations for the Bain path of clean iron have allowed us to investigate the different stable and/or metastable phases of iron according to the energetic of the structures. Interstitial hydrogen hosted on O sites becomes a source of large internal stress that can be released by a body-centered tetragonal deformation that fits naturally with Bain's mechanism. DFT calculations show that the bcc phase is deformed until it reaches an AF-type I phase with  $c/a = 1.5$  (close to the fcc crystal structure). It is favorable for the system to continue deforming to reach a paramagnetic minimum with hexagonal symmetry ( $c/a = 1.6$  and  $\gamma = 60^\circ$ ). This scenario agrees with current ideas about the Earth's core composition under extreme external pressure. Tsuchiya and Fujibuchi have considered the effect of substitutional Si on iron under large pressures [29]. They also conclude that kinetic barriers between bcc and fcc phases disappear under external pressure. In their case, however, the substitutional Si plays a minor role on the physical origin of this effect, probably because an interstitial position increases the internal stress more than a substitutional one. The internal strain introduced by interstitial hydrogen increases the potential energy; this can be used to excite phonons and can propagate through the lattice as an excess vibrational kinetic energy. It is known that the  $\gamma$  to  $\alpha$  transformation happens fast up to a critical temperature,  $M_s$ , but for higher temperatures it is slowed by competition with a different process. Our calculations show that such a martensitic transformation should compete with the formation of an  $\epsilon$  phase

favoured by the accumulation of interstitials in octahedral sites. This process inhibits the  $\gamma$  to  $\alpha$  phase transition, because small nucleation seeds are formed that will grow by attracting further hydrogen diffusing fast at high temperatures.

## ACKNOWLEDGMENTS

This work has been financed by the Spanish MICINN (MAT2008-1497 and BIA2010-18863), and MEC (CSD2007-41 "NANOSELECT" and "SEDUREC").

## REFERENCES

- [1] Eliaz, N., et al., *Characteristics of hydrogen embrittlement, stress corrosion cracking and tempered martensite embrittlement in high-strength steels*. Engineering Failure Analysis, 2002. **9**(2): p. 167-184.
- [2] Elices, M., et al., *The cohesive zone model: advantages, limitations and challenges*. Engineering Fracture Mechanics, 2002. **69**(2): p. 137-163.
- [3] Liang, Y., P. Sofronis, and N. Aravas, *On the effect of hydrogen on plastic instabilities in metals*. Acta Materialia, 2003. **51**(9): p. 2717-2730.
- [4] Sanchez, J., et al., *Stress corrosion cracking mechanism of prestressing steels in bicarbonate solutions*. Corrosion Science, 2007. **49**(11): p. 4069-4080.
- [5] Elices, M., et al., *Hydrogen embrittlement of steels for prestressing concrete: The FIP and DIBt tests*. Corrosion, 2008. **64**(2): p. 164-174.
- [6] Norskov, J.K., *COVALENT EFFECTS IN THE EFFECTIVE-MEDIUM THEORY OF CHEMICAL-BINDING - HYDROGEN HEATS OF SOLUTION IN THE 3D-METALS*. Physical Review B, 1982. **26**(6): p. 2875-2885.
- [7] Elsasser, C., et al., *Ab initio study of iron and iron hydride: I. Cohesion, magnetism and electronic structure of cubic Fe and FeH*. Journal of Physics-Condensed Matter, 1998. **10**(23): p. 5081-5111.
- [8] Juan, A. and R. Hoffmann, *Hydrogen on the Fe(110) surface and near bulk bcc Fe*

- vacancies - A comparative bonding study.* Surface Science, 1999. **421**(1-2): p. 1-16.
- [9] Jiang, D.E. and E.A. Carter, *Diffusion of interstitial hydrogen into and through bcc Fe from first principles.* Physical Review B, 2004. **70**(Copyright (C) 2009 The American Physical Society): p. 064102.
- [10] Gong, X.G., Z. Zeng, and Q.Q. Zheng, *ELECTRONIC-STRUCTURE OF LIGHT IMPURITIES IN ALPHA-Fe AND V.* Journal of Physics-Condensed Matter, 1989. **1**(41): p. 7577-7582.
- [11] Puska, M.J. and R.M. Nieminen, *Theory of hydrogen and helium impurities in metals.* Physical Review B, 1984. **29**(10): p. 5382.
- [12] Antonov, V.E., et al., *Neutron diffraction investigation of the dhcp and hcp iron hydrides and deuterides.* Journal of Alloys and Compounds, 1998. **264**(1-2): p. 214-222.
- [13] Antonov, V.E., et al., *Crystal structure and magnetic properties of high-pressure phases in the Fe---H and Fe---Cr---H systems.* International Journal of Hydrogen Energy, 1989. **14**(6): p. 371-377.
- [14] Antonov, V.E., I.T. Belash, and E.G. Ponyatovsky, *T-P phase diagram of the Fe---H system at temperatures to 450°C and pressures to 6.7 GPa.* Scripta Metallurgica, 1982. **16**(2): p. 203-208.
- [15] Castellote, M., et al., *Hydrogen embrittlement of high-strength steel submitted to slow strain rate testing studied by nuclear resonance reaction analysis and neutron diffraction.* Nuclear Instruments and Methods in Physics Research Section B: Beam Interactions with Materials and Atoms, 2007. **259**(2): p. 975-983.
- [16] Kiuchi, K. and R.B. McLellan, *THE SOLUBILITY AND DIFFUSIVITY OF HYDROGEN IN WELL-ANNEALED AND DEFORMED IRON.* Acta Metallurgica, 1983. **31**(7): p. 961-984.
- [17] Sanchez, J., et al., *Hydrogen Embrittlement of High Strength Steels.* Diffusion in Materials - Dimat2008, 2009. **289-292**: p. 203-209.
- [18] Sanchez, J., et al., *Hydrogen in alpha-iron: Stress and diffusion.* Physical Review B (Condensed Matter and Materials Physics), 2008. **78**(1): p. 014113.
- [19] Bain, E.C., *The nature of martensite.* Transactions of the American Institute of Mining and Metallurgical Engineers, 1924. **70**: p. 25-46.
- [20] Clark, S.J., et al., *First principles methods using CASTEP.* Zeitschrift Fur Kristallographie, 2005. **220**(5-6): p. 567-570.
- [21] Monkhorst, H.J. and J.D. Pack, *SPECIAL POINTS FOR BRILLOUIN-ZONE INTEGRATIONS.* Physical Review B, 1976. **13**(12): p. 5188-5192.
- [22] Vanderbilt, D., *SOFT SELF-CONSISTENT PSEUDOPOTENTIALS IN A GENERALIZED EIGENVALUE FORMALISM.* Physical Review B, 1990. **41**(11): p. 7892-7895.
- [23] Perdew, J.P., K. Burke, and M. Ernzerhof, *Generalized gradient approximation made simple.* Physical Review Letters, 1996. **77**(18): p. 3865-3868.
- [24] Vökl, J. and H. Wipf, *Diffusion of hydrogen in metals.* Hyperfine Interactions, 1981. **8**(4): p. 631-637.
- [25] Hiroi, T., Y. Fukai, and K. Mori, *The phase diagram and superabundant vacancy formation in Fe-H alloys revisited.* Journal of Alloys and Compounds, 2005. **404-406**: p. 252-255.
- [26] Sanchez, J., et al., *Ab initio molecular dynamics simulation of hydrogen diffusion in alpha -iron.* Physical Review B, 2010. **81**(13): p. 132102.
- [27] Castedo, A., et al., *Ab initio study of the cubic-to-hexagonal phase transition promoted by interstitial hydrogen in iron.* Physical Review B, 2011. **84**(9): p. 094101.
- [28] Oriani, R.A., *MECHANISTIC THEORY OF HYDROGEN EMBRITTEMENT OF STEELS.* Berichte Der Bunsen-Gesellschaft Fur Physikalische Chemie, 1972. **76**(8): p. 848-857.
- [29] Tsuchiya, T. and M. Fujibuchi, *Effects of Si on the elastic property of Fe at Earth's*

*inner core pressures: First principles study.* Physics of the Earth and Planetary Interiors, 2009. **174**(1-4): p. 212-219.